

An Odd Estimator for Shapley Values

Fabian Fumagalli¹ Landon Butler² Justin Singh Kang² Kannan Ramchandran² R. Teal Witter³

Abstract

The Shapley value is a ubiquitous framework for attribution in machine learning, encompassing feature importance, data valuation, and causal inference. However, its exact computation is generally intractable, necessitating efficient approximation methods. While the most effective and popular estimators leverage the *paired sampling* heuristic to reduce estimation error, the theoretical mechanism driving this improvement has remained opaque. In this work, we provide an elegant and fundamental justification for paired sampling: we prove that the Shapley value depends *exclusively* on the odd component of the set function, and that paired sampling orthogonalizes the regression objective to filter out the irrelevant even component. Leveraging this insight, we propose OddSHAP, a novel consistent estimator that performs polynomial regression solely on the odd subspace. By utilizing the Fourier basis to isolate this subspace and employing a proxy model to identify high-impact interactions, OddSHAP overcomes the combinatorial explosion of higher-order approximations. Through an extensive benchmark evaluation, we find that OddSHAP achieves state-of-the-art estimation accuracy.

1. Introduction

As machine learning models are increasingly deployed in high-stakes domains—from healthcare and finance to criminal justice—the need to understand their decision-making processes has become paramount (Doshi-Velez & Kim, 2017). To address the opacity of these complex systems, the Shapley value has emerged as the *de facto* standard framework for explanation. Its rigorous game-theoretic foundation has made it ubiquitous across distinct tasks, including

¹LMU Munich, MCML ²Department of Electrical Engineering and Computer Science, UC Berkeley ³Mathematical Sciences Department, Claremont McKenna College. Correspondence to: Fabian Fumagalli <f.fumagalli@lmu.de>, R. Teal Witter <rtealwitter@cmc.edu>.

Preprint. February 3, 2026.

attributing model predictions to input features (Strumbelj & Kononenko, 2010; Lundberg & Lee, 2017), quantifying the contribution of training points to model performance (Ghorbani & Zou, 2019), and estimating the causal effect of variables in structural causal models (Janzing et al., 2020; Heskes et al., 2020).

Let d denote the number of players, indexed by $[d] = \{1, \dots, d\}$. We define a value function $f : 2^{[d]} \rightarrow \mathbb{R}$ that assigns a scalar payoff $f(S)$ to every coalition $S \subseteq [d]$. This abstraction unifies various attribution tasks; depending on the context, $f(S)$ may represent: The prediction of a model masked to only include features in S . The loss of a model trained exclusively on the data points in S . The expected outcome of a structural causal model under an intervention on the variables in S .

In all these settings and more, the value function f implicitly encodes complex higher-order interactions across the 2^d possible subsets. To disentangle these dynamics and attribute the total value to individual players, we turn to the Shapley value. It offers a principled attribution framework, uniquely characterized as the only method satisfying the axioms of *efficiency*, *symmetry*, *dummy*, and *linearity* (Shapley, 1953). For any player $i \in [d]$, the Shapley value of f is defined as the weighted average of marginal contributions:

$$\phi_i(f) = \sum_{S \subseteq [d] \setminus \{i\}} p_{|S|} [f(S \cup \{i\}) - f(S)], \quad (1)$$

where $p_\ell = \frac{1}{d} \binom{d-1}{\ell}^{-1}$. Computing Equation (1) directly involves summing exponentially many terms, rendering exact evaluation intractable for general functions f .

Consequently, exact computation is generally feasible only when the model has exploitable structure (Rozemberczki et al., 2022). This has led to efficient, model-specific algorithms for decision trees ensembles, including TreeSHAP (Lundberg et al., 2020c; Yu et al., 2022) and interaction extensions (Zern et al., 2023; Muschalik et al., 2024c). Similar methods exist for linear (Strumbelj & Kononenko, 2014) and product-kernel models (Mohammadi et al., 2025a), Gaussian processes (Mohammadi et al., 2025b), graph neural networks (Muschalik et al., 2025), and KNN-based data valuation (Jia et al., 2019; Wang et al., 2023; 2024).

Without such structure, one must rely on estimation given a query budget m to evaluate f . Because Shapley values

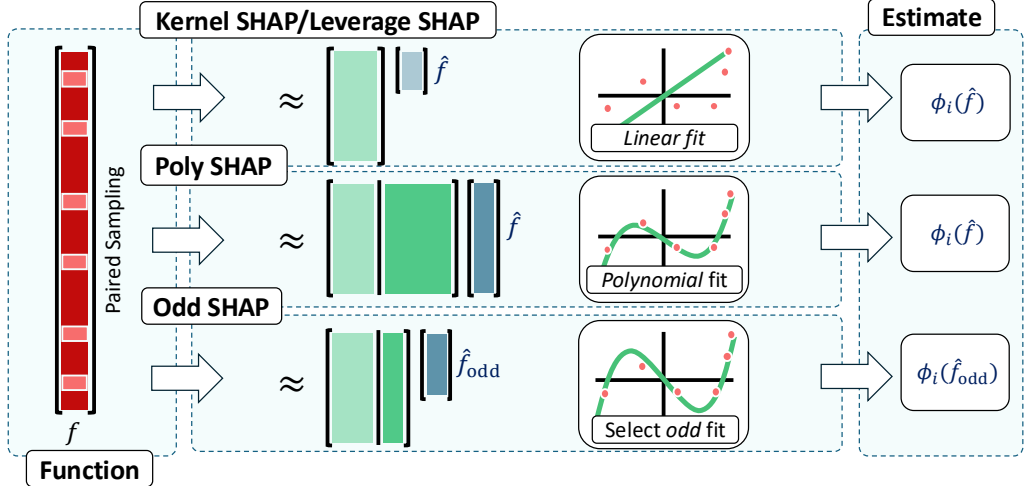


Figure 1. OddSHAP balances expressive power with efficiency by only fitting the *odd* component of the value function.

are widely deployed, a diverse array of estimators has been developed, ranging from Monte Carlo and permutation sampling methods (Castro et al., 2009; Strumbelj & Kononenko, 2014) to regression-based approaches (Lundberg & Lee, 2017). This work focuses on this general model-agnostic setting, where no specific structure of f is assumed.

1.1. Surrogate Estimators

The most effective estimators typically rely on function class approximations: they fit a *structured* surrogate model $\hat{f} \approx f$ and return its exact Shapley values, $\phi_i(\hat{f})$, as the estimate. Crucially, the function class must be structured enough that exactly computing the Shapley values of \hat{f} is efficient.

KernelSHAP (Lundberg & Lee, 2017) and LeverageSHAP (Musco & Witter, 2025) can be viewed through this lens; they exploit a specific weighted linear regression problem whose coefficients recover the exact Shapley values (Charnes et al., 1988). Consequently, these estimators satisfy a *consistency* property: as the sample budget approaches the full coalition space ($m \rightarrow 2^d$), they converge to the true Shapley values. Although practical budgets m are often orders of magnitude smaller than 2^d , this theoretical guarantee appears to be a crucial driver of estimation performance.

Recent advancements have sought to extend this regression framework to more expressive function classes. Methods such as FourierSHAP (Gorji et al., 2025), ProxySPEX (Butler et al., 2025), and RegressionMSR (Witter et al., 2025b) replace the linear basis with sparse Fourier representations or gradient boosted trees (GBTs). If the model class is correctly specified—i.e., if f is truly an exact sparse Fourier function or a tree ensemble—the best approximation \hat{f} coincides with f , ensuring that $\phi_i(\hat{f})$ is consistent.

However, in the general setting, f rarely falls within these restricted classes. Consequently, simple proxy-based esti-

mates are subject to model misspecification bias; even with an infinite query budget, $\phi_i(\hat{f})$ may not converge to $\phi_i(f)$. RegressionMSR addresses this limitation by introducing a residual adjustment term that makes its final estimate consistent, achieving significantly higher accuracy in the large- m regime compared to unadjusted proxy methods.

Recent work has extended the linear regression strategy of KernelSHAP and LeverageSHAP to polynomial regression (Fumagalli et al., 2026). Like both linear methods, the resulting PolySHAP estimator is consistent: Fumagalli et al. (2026) show that the Shapley values of the best *polynomial* approximation to f —under a specific weighting and constraint—are the Shapley values of f itself. While PolySHAP demonstrates superior performance by capturing higher-order interactions, it faces a scalability bottleneck; the computational cost of the regression scales quadratically with the size of the polynomial basis.

1.2. Our Work

Our work aims to circumvent this complexity barrier while retaining the expressive power and consistency of higher-order approximations. To achieve this, we exploit a fundamental structural property: the decomposition of the value function into odd and even components.

A set function f is *odd* if $f(S) = -f(S^c)$ and *even* if $f(S) = f(S^c)$ for all $S \subseteq [d]$, where $S^c := [d] \setminus S$ is the complement. Every f admits a unique decomposition into odd and even components, $f = f_{\text{odd}} + f_{\text{even}}$, with

$$f_{\text{odd}}(S) = \frac{f(S) - f(S^c)}{2}; \quad f_{\text{even}}(S) = \frac{f(S) + f(S^c)}{2}.$$

Crucially, the Shapley value depends *exclusively* on the odd component of the value function:

$$\phi_i(f) = \phi_i(f_{\text{odd}}) \quad \forall i \in [d].$$

Table 1. Average MSE for Shapley value estimators with $m \approx 100d$. OddSHAP achieves the lowest average rank.

m	DistilBERT ($d = 14$)	Estate ($d = 15$)	VIT16 ($d = 16$)	Cancer ($d = 30$)	CG60 ($d = 60$)	IL60 ($d = 60$)	NHANES ($d = 79$)	Crime ($d = 101$)	Avg. Rank
	1591	1857	1895	2315	5521	5521	5864	11126	—
MSR	7.5×10^{-4}	2.8×10^{-2}	1.2×10^{-4}	2.2×10^{-2}	2.1×10^{-3}	3.5×10^{-3}	5.6×10^{-2}	3.6×10^1	6.38
SVARM	3.7×10^{-4}	3.3×10^{-2}	5.7×10^{-5}	3.5×10^{-3}	9.7×10^{-4}	2.2×10^{-3}	4.6×10^{-2}	1.5×10^1	5.38
PermutationSampling	6.2×10^{-4}	5.3×10^{-3}	1.2×10^{-4}	1.1×10^{-4}	1.4×10^{-4}	1.3×10^{-4}	3.7×10^{-3}	2.7×10^0	4.62
3-PolySHAP	8.0×10^{-5}	3.2×10^{-7}	3.8×10^{-5}	4.0×10^{-5}					3.00
LeverageSHAP	7.7×10^{-5}	3.4×10^{-4}	3.5×10^{-5}	3.2×10^{-5}	2.5×10^{-5}	2.6×10^{-5}	7.0×10^{-4}	7.5×10^{-1}	2.88
RegressionMSR	3.1×10^{-5}	1.3×10^{-5}	1.0×10^{-5}	3.0×10^{-4}	7.6×10^{-5}	9.7×10^{-6}	2.7×10^{-4}	5.6×10^{-1}	2.25
OddSHAP	5.2×10^{-5}	6.1×10^{-5}	1.5×10^{-5}	2.3×10^{-5}	6.4×10^{-6}	2.3×10^{-6}	4.6×10^{-5}	1.5×10^{-1}	1.50

This insight suggests a targeted estimation strategy: rather than approximating the full function f —which entails learning potentially complex but irrelevant even structures—we can restrict our approximation to the odd component, $\hat{f}_{\text{odd}} \approx f_{\text{odd}}$, and directly compute $\phi_i(\hat{f}_{\text{odd}})$.

Remarkably, this insight clarifies the theoretical mechanism behind *paired sampling*, a popular heuristic in which every sampled coalition S is paired with its complement S^c . While paired sampling is known to greatly improve estimation performance (Covert & Lee, 2021b; Mitchell et al., 2022; Olsen & Jullum, 2026), a general theoretical justification has remained elusive. Mayer & Wüthrich (2025) proved that KernelSHAP with paired sampling exactly recovers Shapley values for value functions with interactions of at most degree 2, but left the analysis of higher-order interactions open. Subsequently, Fumagalli et al. (2026) demonstrated that a first-order polynomial approximation with paired sampling is equivalent to a second-order approximation, conjecturing a general pattern: that for odd k , an order- k fit with paired sampling is equivalent to order- $(k+1)$. We answer this conjecture in the affirmative and provide a fundamental explanation: paired sampling orthogonalizes the regression problem, separately fitting the odd and even components of f . Since the Shapley value of the even component vanishes, paired sampling effectively acts as a filter, isolating the signal relevant to the Shapley value.

Beyond elucidating the mechanics of paired sampling, we leverage this decomposition to design a more precise Shapley value estimator. Our objective is to reduce the computational complexity of polynomial regression by restricting the model solely to odd terms. However, the standard *unanimity basis*—employed by KernelSHAP, LeverageSHAP, and PolySHAP—is ill-suited for this task, as its individual basis functions do not cleanly decouple into odd and even components. To overcome this, we reformulate the regression problem in the *Fourier basis*. This basis offers a decisive structural advantage: a basis function is odd if and only if its interaction order is odd. Specifically, Fourier terms of odd cardinality are odd functions, while those of even cardinality are even. Consequently, we can efficiently isolate the relevant signal by restricting the polynomial regression exclusively to odd-order Fourier terms.

Even within the restricted odd subspace, the number of candidate terms remains prohibitive; for example, there are $\binom{d}{3}$

distinct third-order interactions. Efficiently identifying the significant few is a challenge addressed by recent interaction detection methods such as SPEX (Kang et al., 2025), FourierSHAP (Gorji et al., 2025), and ProxySPEX (Butler et al., 2025), which learn sparse approximations in the Fourier domain. Leveraging the efficiency of fitting decision trees, we incorporate ProxySPEX as a selection subroutine.

Our proposed algorithm, **OddSHAP**, proceeds in two stages: first, it fits a GBT to the sampled coalitions to identify the dominant odd-order Fourier coefficients; second, it solves the polynomial regression problem restricted to this selected basis. Unlike pure proxy methods, OddSHAP produces a consistent estimator that retains the expressive power of higher-order polynomials. As demonstrated in Figure 2 and Table 1, this hybrid approach achieves state-of-the-art estimation accuracy across a range of standard benchmarks.

Our contributions can be summarized as follows:

- Theoretical Unification of Paired Sampling:** Leveraging the insight that Shapley values depends strictly on the odd component of the value function, we provide the first general theoretical justification for the widely used paired sampling heuristic, proving that it implicitly decouples the regression problem into independent odd and even objectives. This result generalizes prior findings limited to low-order interactions, resolving open questions regarding the heuristic’s effectiveness.
- The OddSHAP Estimator:** We propose OddSHAP, a consistent estimator that performs polynomial regression exclusively on a sparse selection of odd-order Fourier basis functions. By filtering out irrelevant even components and identifying high-impact interactions via a proxy model, OddSHAP retains the expressive power of higher-order polynomials without incurring their prohibitive combinatorial cost.
- State-of-the-Art Performance:** Through extensive experiments on standard benchmarks, we demonstrate that OddSHAP achieves state-of-the-art estimation accuracy. It significantly outperforms higher-order PolySHAP in terms of computational efficiency and surpasses the prior state-of-the-art method, Regression-MSR, in estimation accuracy.

2. Prior Work on Regression Formulations

In this section, we review the notation and results needed to present our work. The foundational mechanism underpinning KernelSHAP, and its improved variant LeverageSHAP, is a *weighted least squares* regression. Both strategies are grounded by a rigorous theoretical guarantee: Charnes et al. (1988) proved that the coefficients of the optimal constrained weighted linear approximation \hat{f} exactly recover the Shapley values of the original function f , i.e., $\phi_i(f) = \phi_i(\hat{f})$.

These frameworks operate using the *unanimity basis*, often referred to as the Möbius basis (Rota, 1964; Grabisch et al., 2016) in combinatorial contexts, where each basis function corresponds to a specific coalition $T \subseteq [d]$. Formally, the unanimity basis functions $u_T : 2^{[d]} \rightarrow \mathbb{R}$ are defined as

$$u_T(S) = \mathbb{1}[T \subseteq S]. \quad (2)$$

Because a full basis expansion involves 2^d terms, fitting the complete set is computationally intractable. Therefore, we restrict our focus to a sparse subset of interactions, denoted by the collection $\mathcal{T} \subseteq 2^{[d]}$.

We define $\mathcal{F}_M(f, \mathcal{T})$ as the class of functions spanned by the unanimity basis restricted to \mathcal{T} , subject to boundary constraints. Specifically, every approximation $g \in \mathcal{F}_M(f, \mathcal{T})$ is constrained to match the ground truth f on the empty and full coalitions, ensuring the efficiency property. Formally,

$$\mathcal{F}_M(f, \mathcal{T}) = \left\{ g = \sum_{T \in \mathcal{T}} u_T \alpha_T : g(S) = f(S), S \in \{\emptyset, [d]\} \right\}$$

Consider the collection of empty and singleton-coalitions $\mathcal{T}_{\leq 1} = \{T \subseteq [d] : |T| \leq 1\}$. Restricting the function to this class allows exact recovery of the Shapley values via a specific weighted and constrained linear regression problem.

Theorem 2.1 (Linear Regression (Charnes et al., 1988)). *Let \hat{f} be the best approximation in $\mathcal{F}_M(f, \mathcal{T}_{\leq 1})$ to f i.e.,*

$$\hat{f} = \operatorname{argmin}_{g \in \mathcal{F}_M(f, \mathcal{T}_{\leq 1})} \sum_{S: \emptyset \subset S \subset [d]} w_{|S|} (f(S) - g(S))^2, \quad (3)$$

where $w_\ell = \frac{1}{\ell(d-\ell)\binom{d}{\ell}}$. Then $\phi_i(f) = \phi_i(\hat{f})$ for all $i \in [d]$.

In cases where the minimizer is not unique, the argmin operator refers to the solution with the minimum ℓ_2 norm. See Musco & Witter (2025) for a modern proof of this result.

Exactly solving the regression requires evaluating f on exponentially many coalitions, KernelSHAP and LeverageSHAP solve an approximate regression problem on only m sampled coalitions. Because of Theorem 2.1, both estimators are *consistent* i.e., they exactly return the Shapley values as the budget m approaches the total number of coalitions 2^d .

Instead of fitting a *linear* approximation, recent Shapley value estimators use richer function classes to more accurately approximate the value function. FourierSHAP (Gorji et al., 2025) uses a sparse Fourier representation, while ProxySPEX (Butler et al., 2025) and RegressionMSR (Witter et al., 2025b) use GBTs. PolySHAP (Fumagalli et al., 2026) fits a *polynomial* regression problem: like the linear regression problem, solving the weighted regression problem with higher-order basis functions also recovers the Shapley values. This has a straightforward geometric interpretation: Shapley values are a *projection* of the value function f onto an affine subspace (the space of linear function satisfying the efficiency constraint), and the weighted polynomial regression is a projection onto a larger subspace. Since intermediate projections onto the larger subspace do not change the output, we have Theorem 2.2.

Theorem 2.2 (Polynomial Regression (Fumagalli et al., 2026)). *Consider any collection of coalitions $\mathcal{T} \supset \mathcal{T}_{\leq 1}$. Let $\hat{f} \in \mathcal{F}_M(f, \mathcal{T})$ be the best approximation to f i.e.,*

$$\hat{f} = \operatorname{argmin}_{g \in \mathcal{F}_M(f, \mathcal{T})} \sum_{S: \emptyset \subset S \subset [d]} w_{|S|} (f(S) - g(S))^2 \quad (4)$$

Then $\phi_i(f) = \phi_i(\hat{f})$ for all $i \in [d]$.

PolySHAP naturally leverages this result: Use m sampled coalitions to solve an approximate version of Equation (4), then return the Shapley values of the approximation, which can be computed quickly via (Harsanyi, 1963):

$$\phi_i(\hat{f}) = \sum_{T \in \mathcal{T}: i \in T} \frac{\alpha_T}{|T|}. \quad (5)$$

While PolySHAP can outperform RegressionMSR for low dimensional settings with low budgets, the algorithm faces a computational bottleneck. As the number of basis vectors grows, finding the best polynomial approximation becomes more computationally intensive: The polynomial regression problem has $|\mathcal{T}|$ columns and m rows, resulting in $O(|\mathcal{T}|^2 m)$ time just to solve the approximate regression problem. For example, if we select the collection up to order- k

$$\mathcal{T}_{\leq k} = \{T \subseteq [d] : |T| \leq k\}, \quad (6)$$

the time complexity is $O(d^{2k} m)$. For $k \geq 2$, the resulting algorithm is prohibitively slow.

3. Our Odd Insights

The goal of our work is to retain the expressive power of the polynomial regression while reducing the complexity of fitting the approximation. The key is to focus on just the *odd* component of the function.

We begin with the observation that only the odd component of a value function is needed to compute its Shapley value. We can then fit an odd approximation \hat{f}_{odd} , retaining the expressive power of the approximation and ignoring the (potentially) expensive process of fitting the even component.

Observation 3.1 (Shapley Values of Odd and Even Functions). *Let $f : 2^{[d]} \rightarrow \mathbb{R}$ be a function. Then, for all $i \in [d]$,*

$$\phi_i(f) = \phi_i(f_{\text{odd}}). \quad (7)$$

Proof. Rearranging Equation 1, we have

$$\phi_i(f) = \sum_{S \subseteq [d]} f(S) (\mathbb{1}[i \in S] p_{|S|-1} - \mathbb{1}[i \notin S] p_{|S|}). \quad (8)$$

Since $f = f_{\text{odd}} + f_{\text{even}}$ and the Shapley value $\phi_i(\cdot)$ is a linear operator, it suffices to show that $\phi_i(f_{\text{even}}) = 0$. We will next rewrite the summation over complementary pairs S and S^c . Without loss of generality, $i \in S$. Then,

$$\begin{aligned} \phi_i(f_{\text{even}}) &= \sum_{S, S^c} f_{\text{even}}(S) p_{|S|-1} - f_{\text{even}}(S^c) p_{|S^c|} \\ &= \sum_{S, S^c} f_{\text{even}}(S) [p_{|S|-1} - p_{|S^c|}], \end{aligned} \quad (9)$$

where the last equality follows because f_{even} is even (i.e., $f_{\text{even}}(S) = f_{\text{even}}(S^c)$). Notice that $|S^c| = d - |S|$. Using the symmetry of the binomial coefficient, it is easy to show that $p_{|S|-1} = p_{d-|S|}$. Then every term in Equation (9) is 0, and the lemma statement follows. \square

3.1. Paired Sampling

While interesting on its own, we can leverage Observation 3.1 to design more efficient Shapley value estimators. Instead of finding an approximation $\hat{f} \approx f$ and returning $\phi_i(\hat{f}) = \phi_i(\hat{f}_{\text{odd}})$, we will fit just the odd component $\hat{f}_{\text{odd}} \approx f_{\text{odd}}$ and directly return $\phi_i(\hat{f}_{\text{odd}})$. Intriguingly, we show that paired sampling is doing just this.

Consider a function class \mathcal{F} . Define $\mathcal{F}_{\text{odd}} := \mathcal{F} \cap \{g : g_{\text{even}}(S) = 0 \forall S\}$ and $\mathcal{F}_{\text{even}} := \mathcal{F} \cap \{g : g_{\text{odd}}(S) = 0 \forall S\}$. We assume the hypothesis class \mathcal{F} is closed under even-odd decomposition, meaning any $g \in \mathcal{F}$ can be uniquely written as $g = g_{\text{odd}} + g_{\text{even}}$, where $g_{\text{odd}} \in \mathcal{F}_{\text{odd}}$ and $g_{\text{even}} \in \mathcal{F}_{\text{even}}$. The Fourier basis discussed in the next section is clearly even-odd decomposable and, by Lemma 3.4, so is the unanimity basis when $\mathcal{T} = \mathcal{T}_{\leq k}$ for some k .

Let \mathcal{S} be a set of paired subsets, i.e., if S is in \mathcal{S} then so is its complement S^c .

Theorem 3.2 (Even-Odd Separation via Paired Sampling). *When using paired samples with a function class that de-*

*composes into odd and even components,*¹

$$\begin{aligned} \operatorname{argmin}_{g \in \mathcal{F}} \sum_{S \in \mathcal{S}} w_{|S|} (f(S) - g(S))^2 \\ = \operatorname{argmin}_{g_{\text{odd}} \in \mathcal{F}_{\text{odd}}} \sum_{S \in \mathcal{S}} w_{|S|} (f_{\text{odd}}(S) - g_{\text{odd}}(S))^2 \\ + \operatorname{argmin}_{g_{\text{even}} \in \mathcal{F}_{\text{even}}} \sum_{S \in \mathcal{S}} w_{|S|} (f_{\text{even}}(S) - g_{\text{even}}(S))^2 \end{aligned} \quad (10)$$

We defer the proof to Appendix B.

Corollary 3.3. *(Frontier Invariance under Unanimity) Under paired sampling, if k is odd,*

$$\phi(\hat{f}_k) = \phi(\hat{f}_{k+1}),$$

where \hat{f}_k is the solution to (10) under class $\mathcal{F}_M(F, \mathcal{T}_{\leq k})$.

This result generalizes the findings of Fumagalli et al. (2026), who established this invariance when $k = 1$. The key observation is that under the unanimity basis, the expansion from odd-degree k to $k + 1$ introduces terms that impact only $\mathcal{F}_{\text{even}}$. See Appendix B for the complete proof.

3.2. Fourier Basis

Our goal is to fit only the *odd* basis functions, but the unanimity basis used in KernelSHAP, LeverageSHAP, and PolySHAP consists of terms that, except at the frontier, are both odd and even. To address this, we will fit functions in the *Fourier* basis.

The Fourier basis consists of functions $\chi_T : 2^{[d]} \rightarrow \mathbb{R}$ where

$$\chi_T(S) = (-1)^{|S \cap T|}. \quad (11)$$

It is easy to check that the function $\chi_T(S)$ is odd if $|T|$ is odd, and even if $|T|$ is even. Analogous to the unanimity basis, we will define a constrained class of functions for fitting the value function f . Let

$$\mathcal{F}_F(f, \mathcal{T}) = \left\{ g = \sum_{T \in \mathcal{T}} \chi_T \beta_T : g(S) = f(S), S \in \{\emptyset, [d]\} \right\}$$

While the unanimity and Fourier bases are distinct, their span on coalitions up to a given order k are equivalent.

Lemma 3.4 (Unanimity and Fourier Equivalence). *For any f , the span of the unanimity and Fourier restricted classes on $\mathcal{T}_{\leq k}$ are the same i.e.,*

$$\mathcal{F}_M(f, \mathcal{T}_{\leq k}) = \mathcal{F}_F(f, \mathcal{T}_{\leq k}). \quad (12)$$

¹When the regression solution is not unique, $+$ denotes Minkowski sum of sets, defined as $A + B = \{g + h \mid g \in A, h \in B\}$.

Algorithm 1 OddSHAP

Require: value function f , sampling budget m , regression variable factor η
 $\mathcal{S} \leftarrow \text{PAIREDSAMPLE}(f, m)$
 $\hat{f}_{\text{GBT}} \leftarrow \text{Fit gradient boosted tree model on } \mathcal{S}$
if $m < d \cdot \eta$ (underdetermined regression)
 return $\phi_1(\hat{f}_{\text{GBT}}), \dots, \phi_d(\hat{f}_{\text{GBT}})$ via TreeSHAP
 $\mathcal{T}_{\text{odd}} \leftarrow \text{ODDINTERACTIONEXTRACT}(\hat{f}_{\text{GBT}}, \lceil \frac{m}{\eta} \rceil)$
 $\hat{f}_{\text{odd}} \leftarrow \underset{g \in \mathcal{F}(f, \mathcal{T}_{\leq 1} \cup \mathcal{T}_{\text{odd}})}{\text{argmin}} \sum_{S \in \mathcal{S}: 0 < |S| < d} w_{|S|} (f(S) - g(S))^2$
return $\phi_1(\hat{f}_{\text{odd}}), \dots, \phi_d(\hat{f}_{\text{odd}})$

We defer the proof to Appendix B.

We show that solving the constrained, weighted regression problem in the Fourier basis recovers the Shapley values.

Theorem 3.5 (Fourier Regression). *Consider any collection of coalitions $\mathcal{T} \supset \mathcal{T}_{\leq 1}$. Consider the best polynomial approximation to f in the Fourier basis on \mathcal{T} :*

$$\hat{f} = \underset{g \in \mathcal{F}_F(f, \mathcal{T})}{\text{argmin}} \sum_{S: \emptyset \subset S \subset [d]} w_{|S|} (f(S) - g(S))^2 \quad (13)$$

Then $\phi_i(f) = \phi_i(\hat{f})$ for all $i \in [d]$.

We defer the proof to Appendix B.

This result establishes that Fourier regression is a consistent estimator, with a computational advantage through Observation 3.1. Since the Fourier basis functions χ_T are strictly odd or even, unlike the unanimity basis functions u_T which are mixed, we can leverage the observation that $\phi_i(f_{\text{even}}) = 0$ to discard even basis terms. We implement this strategy in our algorithm *OddSHAP*.

4. OddSHAP

Algorithm 1 presents OddSHAP in three steps:

1. **Paired Sampling:** We generate pairs (S, S^c) to facilitate even-odd separation.
2. **Interaction Screening:** We fit a GBT to the samples and extract a candidate set \mathcal{T}_{odd} of odd coefficients using ProxySPEX (Butler et al., 2025).
3. **Sparse Odd Regression:** We solve the weighted least squares problem restricted to $\mathcal{T}_{\leq 1} \cup \mathcal{T}_{\text{odd}}$ and return the exact Shapley values of the resulting approximation.

We compute the Shapley values of the resulting approxima-

tion \hat{f}_{odd} :

$$\phi_i(\hat{f}_{\text{odd}}) = -2 \sum_{\substack{T \in \mathcal{T}: i \in T \\ |\mathcal{T}| \text{ odd}}} \frac{\beta_T}{|\mathcal{T}|}. \quad (14)$$

We describe the details of the sampling and regression solver in Section C.

Controlling Higher-Order Terms The set of odd candidate interactions, \mathcal{T}_{odd} , serves as the support for our subsequent regression. Recent works have demonstrated that machine-learned value functions can often be well-approximated by a small number of Fourier interactions (Kang et al., 2025; Butler et al., 2025; Gorji et al., 2025). As we later illustrate in Figure 4, this sparsity can be exploited to significantly improve Shapley value estimation. To construct \mathcal{T}_{odd} , following ProxySPEX (Butler et al., 2025), we fit a GBT to our samples and extract the odd-sized Fourier interactions with the highest magnitudes. We set the size of this candidate set to $\lceil m/\eta \rceil$, for a chosen factor η , ensuring the number of higher-order terms scales with the available sampling budget. In regimes where the sampling budget m is insufficient to fit even the linear terms (i.e. $m < d \cdot \eta$), we revert to the GBT estimates directly using TreeSHAP (Lundberg et al., 2020a), relying on the ensemble’s inherent regularization to provide a stable approximation.

Computational Complexity The computational cost of OddSHAP is primarily driven by the evaluation time T_m of f , which typically dominates when querying complex black-box functions. The subsequent estimation process involves fitting a GBT proxy and solving a sparse regression. Fitting the GBT takes $O(N_{\text{trees}} \cdot m \cdot d)$, while extracting the Fourier representation is efficient at $O(N_{\text{trees}} \cdot 2^L \cdot L)$ for maximum tree depth L . Once the support \mathcal{T} is identified, solving the regression requires $O(|\mathcal{T}|^2 m)$ time, followed by an $O(d \cdot |\mathcal{T}|)$ step to compute the Shapley values. By adaptively constructing the support size as $|\mathcal{T}| = d + \lceil m/\eta \rceil$, OddSHAP ensures the estimation overhead scales polynomially with the budget m and dimension d , rather than the combinatorial $O(d^k)$ scaling of the fixed-order polynomial method PolySHAP. With standard hyperparameters ($\eta = 10, L = 10$), the total runtime is approximately

$$T_m + O(N_{\text{trees}} \cdot m \cdot d + (d + m/\eta)^2 m), \quad (15)$$

keeping the method tractable even for high-dimensional inputs. See Appendix D for empirical runtime analysis.

5. Experiments

To empirically validate OddSHAP, we approximate Shapley values on 8 value functions for local explanations of 30 randomly selected predictions, as listed in Table 2.

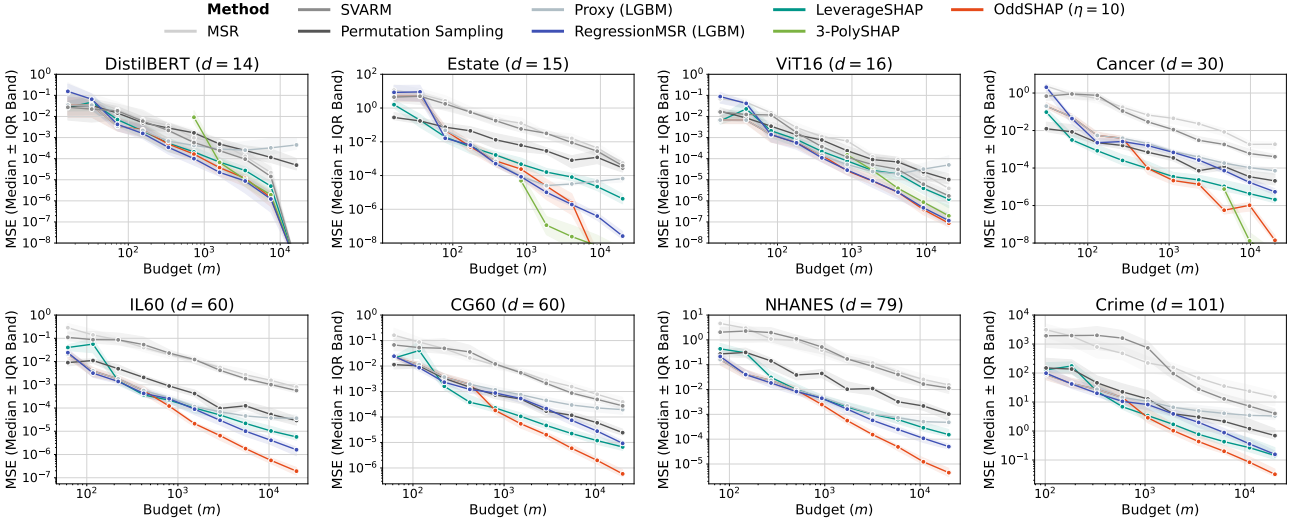


Figure 2. Approximation quality measured by MSE (median with interquartile range) for Shapley value estimators with paired sampling.

Deep Learning Value Functions We utilize the ViT-16 and DistilBERT value functions provided by the `shapiq` library (Muschalik et al., 2024b). For the image domain, the ViT-16 benchmark classifies ImageNet (Deng et al., 2009) samples using a Vision Transformer; the input is segmented into a 4×4 grid of super-patches, resulting in $d = 16$ players. For the text domain, the DistilBERT benchmark (Sanh et al., 2019) predicts sentiment on IMDB (Maas et al., 2011) review excerpts comprising $d = 14$ tokens. Both benchmarks employ baseline imputation, allowing us to compute exact ground-truth Shapley values via exhaustive summation.

Tabular Value Functions For tabular datasets, we train XGBoost classifiers (Chen & Guestrin, 2016) and define the value function via interventional feature perturbation (marginal expectation) estimated using 50 background instances. Ground-truth Shapley values for these models are obtained using the exact interventional TreeSHAP algorithm (Lundberg et al., 2020b).

Estimators We evaluate all methods with m coalitions ranging from $d + 1$ to $\min(2^d, 20000)$, which are sampled according to equal probabilities over coalition sizes and correspond to leverage scores (Musco & Witter, 2025). We compare OddSHAP- η with $\eta = 10$ against *Permutation Sampling* (Castro et al., 2009), *SVARM* (Kolpaczki et al., 2024), *MSR* (Wang & Jia, 2023), i.e. *Unbiased KernelSHAP* (Covert & Lee, 2021a; Fumagalli et al., 2023), and *LeverageSHAP* (Musco & Witter, 2025), which improves KernelSHAP (Lundberg & Lee, 2017) and corresponds to OddSHAP without interactions. We further compare against the proxy-based methods *RegressionMSR* (Witter et al., 2025a) and *Proxy* (LGBM), which corresponds to RegressionMSR

without adjustment, or equivalently *ProxySPEX* (Butler et al., 2025) using all Fourier interactions. All proxy-based methods, including *ProxySPEX* used by OddSHAP, use the same LightGBM (Ke et al., 2017) proxy with default configurations and maximum depth set to 10.

We report *mean-squared error (MSE)* using the median across explained instances and the interquartile range (IQR). We provide our code in the supplementary material, and additional details, metrics and results are provided in Appendix D.

5.1. Approximation Quality of OddSHAP

In practice, the primary computational bottleneck for Shapley value estimation is the cost of evaluating f . Depending on the framework, these evaluations vary in complexity, ranging from simple model predictions (Lundberg & Lee, 2017) to the estimation of conditional distributions (Frye et al., 2021), and even complete model retraining (Strumbelj & Kononenko, 2010; Wang & Jia, 2023). Therefore, we first evaluate the performance of the approximation methods with respect to the number of queries to f .

Figure 2 reports the MSE of OddSHAP and the baselines with respect to the budget m in log-scale. For the low-dimensional value functions, DistilBERT, Estate, and ViT16, OddSHAP yields the same performance as Regression-MSR, which is the best baseline. For all moderate- to high-dimensional value functions, Cancer, IL60, CG60, NHANES, and Crime, OddSHAP clearly outperforms all baselines when having sufficient budget ($m > \eta \cdot d$) to detect and model interactions. In low sample budget scenarios, OddSHAP coincides with *Proxy* (LGBM), and yields comparable results with *RegressionMSR* or *LeverageSHAP*. We

Table 2. Value functions.

d	ID	Source	Domain
14	DistilBERT	shapiq (Muschalik et al., 2024a)	language
15	Estate	Yeh & Hsu (2018)	tabular
16	ViT16	shapiq (Muschalik et al., 2024a)	image
30	Cancer	Street et al. (1993)	tabular
60	CG60	shap (Lundberg & Lee, 2017)	synthetic
60	IL60	shap (Lundberg & Lee, 2017)	synthetic
79	NHANES	Dinh et al. (2019)	tabular
101	Crime	Redmond (2011)	tabular

conclude that OddSHAP yields state-of-the-art performance across all our value functions.

5.2. Ablation of Evaluation Costs

To simulate diverse real-world applications, we vary the evaluation cost of f as $T_1 \in \{0.001, 0.01, 0.1, 1\}$ seconds per evaluation. Although we evaluate f sequentially, we note that in practice, evaluation costs can be amortized through parallelization. Figure 3 reports the MSE (median with IQR) for the runtime of all algorithms and the smallest cost ($T_1 = 0.001$ s). We observe a similar pattern as in Figure 2: OddSHAP outperforms existing baselines. Results for other cost settings and datasets are provided in Section D.

5.3. Ablation of Interaction Sparsity

Figure 4 illustrates the impact of $|\mathcal{T}_{\text{odd}}|$ on the accuracy of Shapley value estimates. We report the MSE Ratio, defined as the Shapley MSE of OddSHAP- η normalized by the error of the interaction-free baseline, LeverageSHAP. Estimates across all value functions were computed under a fixed budget of 10,000 samples, and we defer additional experiments under 5,000 and 20,000 samples to Appendix D, along with results for the Estate value function (omitted here due to outlier improvements).

Across all datasets, we initially observe a strong decrease in the MSE Ratio as the number of odd interactions increases, validating that incorporating influential interactions significantly improves estimation over the interaction-free baseline. Specifically, with 1,000 interactions ($\eta = 10$), we observe at least a $6\times$ reduction in error for all value functions and up to a $62\times$ reduction for one value function (Cancer). However, incorporating too many interactions eventually induces overfitting, reversing these gains.

6. Discussion

We introduce OddSHAP, a state-of-the-art algorithm for computing Shapley values that outperforms all prior algorithms in our experiments for most reasonable budget constraints across a large range of feature dimensions. OddSHAP is based on a theoretical insight: Shapley values depend only on the odd component of the value function. In

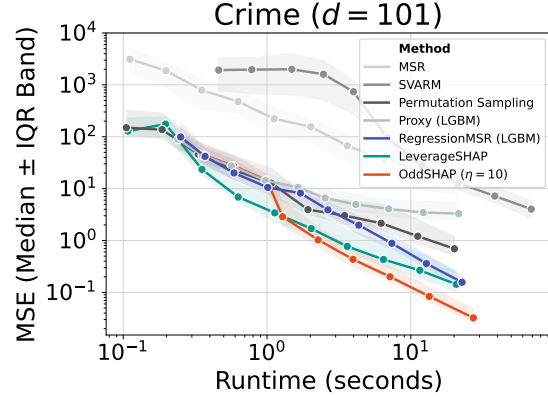


Figure 3. Approximation quality measured by MSE (median with interquartile range) and total runtime in seconds for a simulated setting with 0.001s per subset evaluation. Similar plots for other datasets appear in Section D.

addition to serving as a basis for the OddSHAP algorithm, this insight provides the first rigorous theoretical basis for the popular heuristic of *paired sampling* used in prior state-of-the-art algorithms, and resolves an open conjecture in Fumagalli et al. (2026).

Limitations and Future Directions Several interesting questions remain. Butler et al. (2025) empirically observes a correlation between even and odd interactions in various machine learning applications. With such correlations, learning the even component of the value function, rather than discarding it, could improve Shapley value estimation. Furthermore, paired sampling increases the *mutual coherence* of samples, which could possibly degrade estimation. Future work could investigate algorithms that exploit an even-odd decomposition without paying this cost of increased mutual coherence.

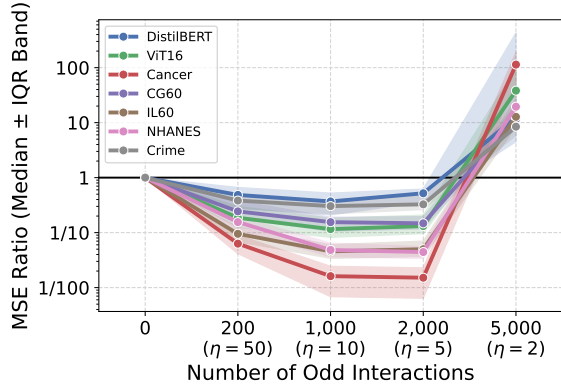


Figure 4. MSE ratio between OddSHAP and LeverageSHAP as a function of the number of selected interactions in OddSHAP, computed under a fixed budget of 10,000 samples.

Impact Statement

This paper presents work whose goal is to advance the field of Machine Learning. There are many potential societal consequences of our work, none which we feel must be specifically highlighted here.

Acknowledgments

This material is based upon work supported by the National Science Foundation Graduate Research Fellowship Program under Grant No. DGE-2146752. Any opinions, findings, and conclusions or recommendations expressed in this material are those of the author(s) and do not necessarily reflect the views of the National Science Foundation.

References

Butler, L., Agarwal, A., Kang, J. S., Erginbas, Y. E., Yu, B., and Ramchandran, K. Proxy-SPEX: Sample-efficient interpretability via sparse feature interactions in LLMs. In *The Thirty-ninth Annual Conference on Neural Information Processing Systems*, 2025. URL <https://openreview.net/forum?id=KI8qan2EA7>.

Castro, J., Gómez, D., and Tejada, J. Polynomial calculation of the Shapley value based on sampling. *Computers & Operations Research*, 36(5):1726–1730, 2009. doi: 10.1016/j.cor.2008.04.004.

Charnes, A., Golany, B., Keane, M., and Rousseau, J. Extremal principle solutions of games in characteristic function form: core, chebychev and shapley value generalizations. In *Econometrics of planning and efficiency*, pp. 123–133. Springer, 1988.

Chen, T. and Guestrin, C. XGBoost: A scalable tree boosting system. In *Proceedings of the 22nd ACM SIGKDD International Conference on Knowledge Discovery and Data Mining (KDD)*, pp. 785–794. ACM, 2016. doi: 10.1145/2939672.2939785.

Covert, I. and Lee, S. Improving KernelSHAP: Practical Shapley Value Estimation Using Linear Regression. In *Proceedings of the International Conference on Artificial Intelligence and Statistics (AISTATS)*, pp. 3457–3465, 2021a.

Covert, I. and Lee, S.-I. Improving kernelshap: Practical shapley value estimation using linear regression. In *International conference on artificial intelligence and statistics*, pp. 3457–3465. PMLR, 2021b.

Deng, J., Dong, W., Socher, R., Li, L., Li, K., and Fei-Fei, L. Imagenet: A large-scale hierarchical image database. In *Proceedings of IEEE Computer Society Conference on Computer Vision and Pattern Recognition (CVPR)*, pp. 248–255, 2009.

Dinh, A., Miertschin, S., Young, A., and Mohanty, S. D. A data-driven approach to predicting diabetes and cardiovascular disease with machine learning. *BMC Medical Informatics Decision Making*, 19(1):211:1–211:15, 2019. doi: 10.1186/S12911-019-0918-5.

Doshi-Velez, F. and Kim, B. Towards a rigorous science of interpretable machine learning. *arXiv preprint arXiv:1702.08608*, 2017.

Frye, C., de Mijolla, D., Begley, T., Cowton, L., Stanley, M., and Feige, I. Shapley explainability on the data manifold. In *Proceedings of the International Conference on Learning Representations (ICLR)*, 2021.

Fumagalli, F., Muschalik, M., Kolpaczki, P., Hüllermeier, E., and Hammer, B. SHAP-IQ: Unified Approximation of any-order Shapley Interactions. In *Proceedings of Advances in Neural Information Processing Systems (NeurIPS)*, 2023.

Fumagalli, F., Witter, R. T., and Musco, C. Polyshap: Extending kernelshap with interaction-informed polynomial regression. *arXiv preprint arXiv:2601.18608*, 2026.

Ghorbani, A. and Zou, J. Y. Data shapley: Equitable valuation of data for machine learning. In *Proceedings of the International Conference on Machine Learning (ICML)*, pp. 2242–2251, 2019.

Gorji, A., Amrollahi, A., and Krause, A. SHAP values via sparse fourier representation. In *The Thirty-ninth Annual Conference on Neural Information Processing Systems*, 2025. URL <https://openreview.net/forum?id=wab4BEAUt6>.

Grabisch, M. *Set Functions, Games and Capacities in Decision Making*, volume 46. Springer International Publishing Switzerland, 2016. ISBN 978-3-319-30690-2. doi: 10.1007/978-3-319-30690-2.

Grabisch, M. et al. *Set functions, games and capacities in decision making*, volume 46. Springer, 2016.

Harsanyi, J. C. A simplified bargaining model for the n-person cooperative game. *International Economic Review*, 4(2):194–220, 1963.

Heskes, T., Sijben, E., Bucur, I. G., and Claassen, T. Causal shapley values: Exploiting causal knowledge to explain individual predictions of complex models. *Advances in neural information processing systems*, 33:4778–4789, 2020.

Janzing, D., Minorics, L., and Blöbaum, P. Feature relevance quantification in explainable AI: A causal problem. In *Proceedings of the International Conference on Artificial Intelligence and Statistics (AISTATS)*, pp. 2907–2916, 2020.

Jia, R., Dao, D., Wang, B., Hubis, F. A., Hynes, N., Gürel, N. M., Li, B., Zhang, C., Song, D., and Spanos, C. J. Towards efficient data valuation based on the shapley value. In *Proceedings of the 22nd International Conference on Artificial Intelligence and Statistics (AISTATS)*, pp. 1167–1176. PMLR, 2019.

Kang, J. S., Butler, L., Agarwal, A., Erginbas, Y. E., Pedarsani, R., Yu, B., and Ramchandran, K. SPEX: Scaling feature interaction explanations for LLMs. In *Forty-second International Conference on Machine Learning*, 2025. URL <https://openreview.net/forum?id=pR1KbAwczl>.

Ke, G., Meng, Q., Finley, T., Wang, T., Chen, W., Ma, W., Ye, Q., and Liu, T. LightGBM: A Highly Efficient Gradient Boosting Decision Tree. In *Proceedings of Advances in Neural Information Processing Systems (NeurIPS)*, pp. 3146–3154, 2017.

Kolpaczki, P., Bengs, V., Muschalik, M., and Hüllermeier, E. Approximating the shapley value without marginal contributions. In *Proceedings of the AAAI Conference on Artificial Intelligence (AAAI)*, pp. 13246–13255, 2024.

Langley, P. Crafting papers on machine learning. In Langley, P. (ed.), *Proceedings of the 17th International Conference on Machine Learning (ICML 2000)*, pp. 1207–1216, Stanford, CA, 2000. Morgan Kaufmann.

Lundberg, S. M. and Lee, S. A Unified Approach to Interpreting Model Predictions. In *Proceedings of Advances in Neural Information Processing Systems (NeurIPS)*, pp. 4765–4774, 2017.

Lundberg, S. M., Erion, G., Chen, H., DeGrave, A., Prutkin, J. M., Nair, B., Katz, R., Himmelfarb, J., Bansal, N., and Lee, S.-I. From local explanations to global understanding with explainable ai for trees. *Nature machine intelligence*, 2(1):56–67, 2020a.

Lundberg, S. M., Erion, G. G., Chen, H., DeGrave, A. J., Prutkin, J. M., Nair, B., Katz, R., Himmelfarb, J., Bansal, N., and Lee, S. From local explanations to global understanding with explainable AI for trees. *Nature Machine Intelligence*, 2(1):56–67, 2020b. doi: 10.1038/s42256-019-0138-9.

Lundberg, S. M., Erion, G. G., Chen, H., DeGrave, A. J., Prutkin, J. M., Nair, B., Katz, R., Himmelfarb, J., Bansal, N., and Lee, S. From local explanations to global understanding with explainable AI for trees. *Nature Machine Intelligence*, 2(1):56–67, 2020c.

Maas, A. L., Daly, R. E., Pham, P. T., Huang, D., Ng, A. Y., and Potts, C. Learning word vectors for sentiment analysis. In *Proceedings of the 49th Annual Meeting of the Association for Computational Linguistics: Human Language Technologies (HLT)*, pp. 142–150, 2011.

Mayer, M. and Wüthrich, M. V. Shapley values: Paired-sampling approximations. *CoRR*, abs/2508.12947, 2025.

Mitchell, R., Cooper, J., Frank, E., and Holmes, G. Sampling permutations for shapley value estimation. *Journal of Machine Learning Research*, 23(43):1–46, 2022.

Mohammadi, M., Chau, S. L., and Muandet, K. Computing exact shapley values in polynomial time for product-kernel methods. *arXiv preprint arXiv:2505.16516*, 2025a.

Mohammadi, M., Muandet, K., Tiddi, I., Teije, A. T., and Chau, S. L. Exact shapley attributions in quadratic-time for fanova gaussian processes. *arXiv preprint arXiv:2508.14499*, 2025b.

Muschalik, M., Baniecki, H., Fumagalli, F., Kolpaczki, P., Hammer, B., and Hüllermeier, E. shapiq: Shapley Interactions for Machine Learning. In *Proceedings of Advances in Neural Information Processing Systems (NeurIPS)*, pp. 130324–130357, 2024a.

Muschalik, M., Baniecki, H., Fumagalli, F., Kolpaczki, P., Hammer, B., and Hüllermeier, E. shapiq: Shapley Interactions for Machine Learning. In *Advances in Neural Information Processing Systems (NeurIPS)*, volume 37, pp. 130324–130357, 2024b.

Muschalik, M., Fumagalli, F., Hammer, B., and Hüllermeier, E. Beyond TreeSHAP: Efficient Computation of Any-Order Shapley Interactions for Tree Ensembles. In *Proceedings of the AAAI Conference on Artificial Intelligence (AAAI)*, pp. 14388–14396, 2024c. doi: 10.1609/aaai.v38i13.29352.

Muschalik, M., Fumagalli, F., Fazzetto, P., Strotherm, J., Hermes, L., Sperduti, A., Hüllermeier, E., and Hammer, B. Exact Computation of Any-Order Shapley Interactions for Graph Neural Networks. In *The Thirteenth International Conference on Learning Representations*, 2025.

Musco, C. and Witter, R. T. Provably Accurate Shapley Value Estimation via Leverage Score Sampling. In *Proceedings of the International Conference on Learning Representations (ICLR)*, 2025.

Olsen, L. H. B. and Jullum, M. Improving the weighting strategy in kernelshap. In Guidotti, R., Schmid, U.,

and Longo, L. (eds.), *Explainable Artificial Intelligence*, pp. 194–218, Cham, 2026. Springer Nature Switzerland. ISBN 978-3-032-08324-1.

Redmond, M. Communities and crime unnormalized, 2011.

Rota, G.-C. On the foundations of combinatorial theory: I. theory of möbius functions. In *Classic Papers in Combinatorics*, pp. 332–360. Springer, 1964.

Rozemberczki, B., Watson, L., Bayer, P., Yang, H., Kiss, O., Nilsson, S., and Sarkar, R. The shapley value in machine learning. In *Proceedings of International Joint Conference on Artificial Intelligence (IJCAI)*, pp. 5572–5579, 2022.

Sanh, V., Debut, L., Chaumond, J., and Wolf, T. Distilbert, a distilled version of bert: smaller, faster, cheaper and lighter. *CoRR*, abs/1910.01108, 2019.

Shapley, L. S. A Value for n-Person Games. In *Contributions to the Theory of Games (AM-28), Volume II*, pp. 307–318. Princeton University Press, 1953.

Street, W. N., Wolberg, W. H., and Mangasarian, O. L. Nuclear feature extraction for breast tumor diagnosis. In *Biomedical image processing and biomedical visualization*, volume 1905, pp. 861–870, 1993.

Strumbelj, E. and Kononenko, I. An Efficient Explanation of Individual Classifications using Game Theory. *Journal of Machine Learning Research*, 11:1–18, 2010. doi: 10.5555/1756006.1756007.

Strumbelj, E. and Kononenko, I. Explaining prediction models and individual predictions with feature contributions. *Knowledge and Information Systems*, 41(3): 647–665, 2014. doi: 10.1007/s10115-013-0679-x.

Štrumbelj, E. and Kononenko, I. Explaining prediction models and individual predictions with feature contributions. *Knowledge and information systems*, 41:647–665, 2014.

Wang, J. T. and Jia, R. Data banzhaf: A robust data valuation framework for machine learning. In Ruiz, F. J. R., Dy, J. G., and van de Meent, J. (eds.), *Proceedings of the International Conference on Artificial Intelligence and Statistics (AISTATS)*, pp. 6388–6421, 2023.

Wang, J. T., Zhu, Y., Wang, Y.-X., Jia, R., and Mittal, P. A privacy-friendly approach to data valuation. In *Advances in Neural Information Processing Systems (NeurIPS)*, volume 37, 2023.

Wang, J. T., Mittal, P., and Jia, R. Efficient data shapley for weighted nearest neighbor algorithms. In *Proceedings of the 27th International Conference on Artificial Intelligence and Statistics (AISSTATS)*, pp. 2557–2565. PMLR, 2024.

Witter, R. T., Liu, Y., and Musco, C. Regression-adjusted monte carlo estimators for shapley values and probabilistic values. *CoRR*, abs/2506.11849, 2025a.

Witter, R. T., Liu, Y., and Musco, C. Regression-adjusted monte carlo estimators for shapley values and probabilistic values. In *The Thirty-ninth Annual Conference on Neural Information Processing Systems*, 2025b. URL <https://openreview.net/forum?id=Qabko39AS5>.

Yeh, I. and Hsu, T. Building real estate valuation models with comparative approach through case-based reasoning. *Applied Soft Computing*, 65:260–271, 2018. doi: 10.1016/J.ASOC.2018.01.029.

Yu, P., Bifet, A., Read, J., and Xu, C. Linear tree shap. In *Advances in Neural Information Processing Systems (NeurIPS)*, volume 35, 2022.

Zern, A., Broelemann, K., and Kasneci, G. Interventional SHAP values and interaction values for piecewise linear regression trees. In *Proceedings of the 37th AAAI Conference on Artificial Intelligence*, volume 37, pp. 11164–11173, 2023.

A. Expanded Table

Table 3. Summary statistics of MSE for Shapley value estimators with $m \approx 100d$. OddSHAP achieves the lowest average rank.

<i>m</i>	DistilBERT ($d = 14$) 1591	Estate ($d = 15$) 1857	VIT16 ($d = 16$) 1895	Cancer ($d = 30$) 2315	CG60 ($d = 60$) 5521	IL60 ($d = 60$) 5521	NHANES ($d = 79$) 5864	Crime ($d = 101$) 11126	Avg. Rank –
MSR									
Mean	7.5×10^{-4}	2.8×10^{-2}	1.2×10^{-4}	2.2×10^{-2}	2.1×10^{-3}	3.5×10^{-3}	5.6×10^{-2}	3.6×10^1	6.38
1st Quartile	1.6×10^{-4}	1.7×10^{-2}	4.4×10^{-5}	1.2×10^{-2}	1.1×10^{-3}	1.9×10^{-3}	2.5×10^{-2}	9.7×10^0	6.25
Median	5.6×10^{-4}	2.8×10^{-2}	1.2×10^{-4}	2.3×10^{-2}	1.6×10^{-3}	2.7×10^{-3}	5.0×10^{-2}	2.4×10^1	6.38
3rd Quartile	8.8×10^{-4}	4.0×10^{-2}	1.8×10^{-4}	2.9×10^{-2}	2.1×10^{-3}	4.5×10^{-3}	8.1×10^{-2}	3.7×10^1	6.38
SVARM									
Mean	3.7×10^{-4}	3.3×10^{-2}	5.7×10^{-5}	3.5×10^{-3}	9.7×10^{-4}	2.2×10^{-3}	4.6×10^{-2}	1.5×10^1	5.38
1st Quartile	6.5×10^{-5}	1.6×10^{-2}	2.6×10^{-5}	2.3×10^{-3}	7.8×10^{-4}	1.6×10^{-3}	2.3×10^{-2}	5.3×10^0	5.25
Median	2.4×10^{-4}	3.2×10^{-2}	5.2×10^{-5}	3.0×10^{-3}	8.7×10^{-4}	1.8×10^{-3}	4.0×10^{-2}	7.2×10^0	5.38
3rd Quartile	4.7×10^{-4}	4.8×10^{-2}	7.5×10^{-5}	4.7×10^{-3}	1.1×10^{-3}	2.4×10^{-3}	6.0×10^{-2}	1.1×10^1	5.38
PermutationSampling									
Mean	6.2×10^{-4}	5.3×10^{-3}	1.2×10^{-4}	1.1×10^{-4}	1.4×10^{-4}	1.3×10^{-4}	3.7×10^{-3}	2.7×10^0	4.62
1st Quartile	2.3×10^{-4}	1.9×10^{-3}	6.2×10^{-5}	5.3×10^{-5}	8.0×10^{-5}	9.1×10^{-5}	2.2×10^{-3}	8.6×10^{-1}	4.88
Median	4.9×10^{-4}	2.9×10^{-3}	9.1×10^{-5}	7.2×10^{-5}	1.2×10^{-4}	1.2×10^{-4}	3.2×10^{-3}	1.2×10^0	4.62
3rd Quartile	8.6×10^{-4}	4.4×10^{-3}	1.6×10^{-4}	1.7×10^{-4}	1.6×10^{-4}	1.9×10^{-4}	5.0×10^{-3}	2.6×10^0	4.62
3-PolySHAP									
Mean	8.0×10^{-5}	3.2×10^{-7}	3.8×10^{-5}	4.0×10^{-5}					3.00
1st Quartile	4.5×10^{-5}	3.1×10^{-8}	1.7×10^{-5}	1.3×10^{-5}					2.50
Median	6.6×10^{-5}	1.1×10^{-7}	2.8×10^{-5}	2.7×10^{-5}					2.75
3rd Quartile	1.1×10^{-4}	3.7×10^{-7}	4.8×10^{-5}	6.2×10^{-5}					2.75
LeverageSHAP									
Mean	7.7×10^{-5}	3.4×10^{-4}	3.5×10^{-5}	3.2×10^{-5}	2.5×10^{-5}	2.6×10^{-5}	7.0×10^{-4}	7.5×10^{-1}	2.88
1st Quartile	3.2×10^{-5}	9.2×10^{-5}	1.9×10^{-5}	1.1×10^{-5}	1.8×10^{-5}	1.3×10^{-5}	4.2×10^{-4}	1.9×10^{-1}	2.75
Median	6.9×10^{-5}	1.6×10^{-4}	2.7×10^{-5}	2.3×10^{-5}	2.2×10^{-5}	2.2×10^{-5}	6.2×10^{-4}	2.7×10^{-1}	2.88
3rd Quartile	1.1×10^{-4}	2.6×10^{-4}	4.3×10^{-5}	4.2×10^{-5}	3.2×10^{-5}	3.2×10^{-5}	8.3×10^{-4}	5.8×10^{-1}	3.00
RegressionMSR									
Mean	3.1×10^{-5}	1.3×10^{-5}	1.0×10^{-5}	3.0×10^{-4}	7.6×10^{-5}	9.7×10^{-6}	2.7×10^{-4}	5.6×10^{-1}	2.25
1st Quartile	1.4×10^{-5}	6.5×10^{-6}	4.4×10^{-6}	1.8×10^{-4}	5.0×10^{-5}	6.1×10^{-6}	1.7×10^{-4}	3.0×10^{-1}	2.50
Median	2.2×10^{-5}	1.0×10^{-5}	8.9×10^{-6}	2.7×10^{-4}	7.4×10^{-5}	1.0×10^{-5}	2.5×10^{-4}	3.6×10^{-1}	2.38
3rd Quartile	4.1×10^{-5}	1.8×10^{-5}	1.2×10^{-5}	4.1×10^{-4}	1.0×10^{-4}	1.2×10^{-5}	3.2×10^{-4}	5.4×10^{-1}	2.25
OddSHAP									
Mean	5.2×10^{-5}	6.1×10^{-5}	1.5×10^{-5}	2.3×10^{-5}	6.4×10^{-6}	2.3×10^{-6}	4.6×10^{-5}	1.5×10^{-1}	1.50
1st Quartile	2.1×10^{-5}	5.8×10^{-6}	6.3×10^{-6}	1.3×10^{-5}	4.4×10^{-6}	1.3×10^{-6}	2.7×10^{-5}	7.6×10^{-2}	1.62
Median	4.8×10^{-5}	4.0×10^{-5}	1.1×10^{-5}	2.0×10^{-5}	6.2×10^{-6}	2.0×10^{-6}	4.2×10^{-5}	9.9×10^{-2}	1.50
3rd Quartile	6.6×10^{-5}	1.0×10^{-4}	2.1×10^{-5}	3.0×10^{-5}	7.6×10^{-6}	2.5×10^{-6}	5.0×10^{-5}	1.5×10^{-1}	1.50

B. Delayed Proofs

Theorem 3.2 (Even-Odd Separation via Paired Sampling). *When using paired samples with a function class that decomposes into odd and even components,²*

$$\operatorname{argmin}_{g \in \mathcal{F}} \sum_{S \in \mathcal{S}} w_{|S|} (f(S) - g(S))^2 = \operatorname{argmin}_{g_{\text{odd}} \in \mathcal{F}_{\text{odd}}} \sum_{S \in \mathcal{S}} w_{|S|} (f_{\text{odd}}(S) - g_{\text{odd}}(S))^2 + \operatorname{argmin}_{g_{\text{even}} \in \mathcal{F}_{\text{even}}} \sum_{S \in \mathcal{S}} w_{|S|} (f_{\text{even}}(S) - g_{\text{even}}(S))^2$$

Proof of Theorem 3.2. Consider the inner summation for a specific pair S and S^c . Since $w_{|S|} = w_{|S^c|}$, we can expand the sum over the pair and apply an even-odd decomposition:

$$\begin{aligned} & (f(S) - g(S))^2 + (f(S^c) - g(S^c))^2 \\ &= (f_{\text{even}}(S) + f_{\text{odd}}(S) - g_{\text{even}}(S) - g_{\text{odd}}(S))^2 + (f_{\text{even}}(S^c) + f_{\text{odd}}(S^c) - g_{\text{even}}(S^c) - g_{\text{odd}}(S^c))^2. \end{aligned} \quad (16)$$

Using the definition of even and odd functions on the complement:

$$(16) = (f_{\text{even}}(S) + f_{\text{odd}}(S) - g_{\text{even}}(S) - g_{\text{odd}}(S))^2 + (f_{\text{even}}(S) - f_{\text{odd}}(S) - g_{\text{even}}(S) + g_{\text{odd}}(S))^2. \quad (17)$$

After expanding and refactoring:

$$\begin{aligned} (17) &= 2(f_{\text{odd}}(S) - g_{\text{odd}}(S))^2 + 2(f_{\text{even}}(S) - g_{\text{even}}(S))^2 \\ &= (f_{\text{odd}}(S) - g_{\text{odd}}(S))^2 + (f_{\text{even}}(S) - g_{\text{even}}(S))^2 + (f_{\text{odd}}(S^c) - g_{\text{odd}}(S^c))^2 + (f_{\text{even}}(S^c) - g_{\text{even}}(S^c))^2, \end{aligned}$$

where the last equation follows by again applying the definition of even and odd functions to half of the terms. Substituting this expression back into the objective and separating the minimization completes the proof. \square

Corollary 3.3 (Frontier Invariance under Unanimity). Under paired sampling, if k is odd,

$$\phi(\hat{f}_k) = \phi(\hat{f}_{k+1}),$$

where \hat{f}_k is the solution to (10) under class $\mathcal{F}_M(F, \mathcal{T}_{\leq k})$.

Proof. By Lemma 3.4, the restricted unanimity class $\mathcal{F}_M(F, \mathcal{T}_{\leq k})$ is equivalent to the Fourier restricted class $\mathcal{F}_F(F, \mathcal{T}_{\leq k})$. We can therefore parameterize the solution space using Fourier coefficients, where the conversion to unanimity coefficients is given by Eq. 2.76 in (Grabisch, 2016):

$$\alpha_S = (-2)^{|S|} \sum_{T \supseteq S} \beta_T. \quad (18)$$

Consider the expansion from degree limit k to $k+1$. By the conversion above, it can be seen that this only introduces Fourier basis terms corresponding to subsets T where $|T| = k+1$. Since k is odd, $k+1$ is even. Thus, the expansion only adds dimensions to the even subspace of the Fourier domain. The subspace of odd-degree Fourier terms remains identical.

By Theorem 3.2, under paired sampling, the optimization of the odd component is independent of the even subspace. Consequently, the odd component of the minimizer remains invariant, and by Observation 3.1, $\phi(\hat{f}_k) = \phi(\hat{f}_{k+1})$. \square

Lemma 3.4 (Unanimity and Fourier Equivalence). *For any f , the span of the unanimity and Fourier restricted classes on $\mathcal{T}_{\leq k}$ are the same i.e.,*

$$\mathcal{F}_M(f, \mathcal{T}_{\leq k}) = \mathcal{F}_F(f, \mathcal{T}_{\leq k}). \quad (19)$$

Proof of Lemma 3.4. First, observe that the constraints $g(S) = f(S), S \in \{\emptyset, [d]\}$ are conditions on the function values, which are independent of the basis representation. Therefore, it suffices to show that the unconstrained spans of the two bases restricted to order k are identical.

²When the regression solution is not unique, $+$ denotes Minkowski sum of sets, defined as $A + B = \{g + h \mid g \in A, h \in B\}$.

Fourier to Unanimity: Assume g is in the unconstrained Fourier class of up to order k (i.e. $\beta_T = 0$ for all $|T| > k$). We apply the conversion from Fourier to unanimity coefficients, given by Eq. 2.76 in (Grabisch, 2016):

$$\alpha_S = (-2)^{|S|} \sum_{T \supseteq S} \beta_T. \quad (20)$$

For any set S such that $|S| > k$, the condition $T \supseteq S$ implies $|T| \geq |S| > k$. Thus, $\beta_T = 0$ for all such T , which implies $\alpha_S = 0$. Thus, g admits a representation in the unanimity class of up to order k .

Unanimity to Fourier: Conversely, assume g is in the unanimity class of up to order k (i.e. $\alpha_S = 0$ for all $|S| > k$). Using the conversion from unanimity to Fourier coefficients from Eq. 2.74 in (Grabisch, 2016):

$$\beta_T = (-1)^{|T|} \sum_{S \supseteq T} \frac{\alpha_S}{2^{|S|}}. \quad (21)$$

It can be seen that any set T such that $|T| > k$ has $\beta_T = 0$. Therefore, g admits a representation in the Fourier class of up to order k .

Since the unconstrained subspaces are identical, and the boundary constraints are basis-independent, we conclude that $\mathcal{F}_M(f, \mathcal{T}_{\leq k}) = \mathcal{F}_F(f, \mathcal{T}_{\leq k})$. \square

Theorem 3.5 (Fourier Regression). *Consider any collection of coalitions $\mathcal{T} \supset \mathcal{T}_{\leq 1}$. Consider the best polynomial approximation to f in the Fourier basis on \mathcal{T} :*

$$\hat{f} = \operatorname{argmin}_{g \in \mathcal{F}_F(f, \mathcal{T})} \sum_{S: \emptyset \subset S \subset [d]} w_{|S|} (f(S) - g(S))^2$$

Then $\phi_i(f) = \phi_i(\hat{f})$ for all $i \in [d]$.

Proof of Theorem 3.5. The proof relies on the nested structure of the regression spaces and the property that orthogonal projections onto nested subspaces can be composed.

First, by Lemma 3.4, the restricted function classes for the unanimity and Fourier bases on $\mathcal{T}_{\leq 1}$ are identical:

$$\mathcal{F}_F(f, \mathcal{T}_{\leq 1}) = \mathcal{F}_M(f, \mathcal{T}_{\leq 1}). \quad (22)$$

Let $\mathcal{V}_{\text{small}} = \mathcal{F}_F(f, \mathcal{T}_{\leq 1})$ denote the affine subspace of additive functions satisfying the boundary constraints. Similarly, let $\mathcal{V}_{\text{large}} = \mathcal{F}_F(f, \mathcal{T})$ denote the affine subspace spanned by the Fourier basis on \mathcal{T} satisfying the same constraints. Since $\mathcal{T}_{\leq 1} \subset \mathcal{T}$, it follows that $\mathcal{V}_{\text{small}} \subset \mathcal{V}_{\text{large}}$.

We define the weighted inner product $\langle g, h \rangle_w = \sum_S w_{|S|} g(S)h(S)$. The regression problem in Equation (13) is equivalent to finding the orthogonal projection of f onto $\mathcal{V}_{\text{large}}$ under this inner product. Let \hat{f} be this solution:

$$\hat{f} = \operatorname{proj}_{\mathcal{V}_{\text{large}}} (f). \quad (23)$$

Similarly, let \hat{g} be the best linear approximation to f (the solution to Equation (3)):

$$\hat{g} = \operatorname{proj}_{\mathcal{V}_{\text{small}}} (f). \quad (24)$$

By the tower property of projections onto nested subspaces, projecting f onto the smaller space $\mathcal{V}_{\text{small}}$ is equivalent to first projecting f onto the larger space $\mathcal{V}_{\text{large}}$, and then projecting the result onto $\mathcal{V}_{\text{small}}$. Therefore:

$$\hat{g} = \operatorname{proj}_{\mathcal{V}_{\text{small}}} (\hat{f}). \quad (25)$$

This implies that \hat{g} is *also* the best linear approximation to \hat{f} .

We now invoke Theorem 2.1. The theorem states that for any function, its Shapley values are exactly recovered by its best linear approximation. Applying this to f and \hat{f} respectively:

1. $\phi_i(f) = \phi_i(\hat{g})$ (Applying Theorem 2.1 to f).
2. $\phi_i(\hat{f}) = \phi_i(\hat{g})$ (Applying Theorem 2.1 to \hat{f}).

Combining these equalities yields $\phi_i(f) = \phi_i(\hat{f})$, completing the proof. \square

C. Sampling and Regressing in OddSHAP

In this appendix, we detail the sampling strategy used in OddSHAP and derive the closed-form constraints required to enforce the efficiency property in the Fourier domain.

C.1. Sampling Strategy

We sample coalitions $S \subseteq [d]$ without replacement, with uniform weights by coalition size. This strategy aligns naturally with the definition of the Shapley value, which equally weights coalitions uniformly by their size. Furthermore, this distribution is theoretically grounded: [Musco & Witter \(2025\)](#) demonstrate that these weights correspond to the leverage scores of the weighted linear regression problem in [Theorem 2.1](#).

This sampling procedure is consistent with the standard implementations of KernelSHAP, LeverageSHAP, and PolySHAP ensuring a fair comparison between estimators.

C.2. Exact Boundary Constraints in the Fourier Domain

A critical requirement for Shapley value estimators is the *efficiency* property, which mandates that the sum of the estimated feature attributions equals the difference between the total payout and the baseline: $\sum \phi_i = f([d]) - f(\emptyset)$. In the regression framework, this is equivalent to constraining the approximation \hat{f} to match the ground truth on the empty and full sets:

$$\hat{f}(\emptyset) = f(\emptyset) \quad \text{and} \quad \hat{f}([d]) = f([d]). \quad (26)$$

Standard implementations of KernelSHAP enforce these constraints “softly” by assigning a very large weight (simulating infinity) to the samples for \emptyset and $[d]$. However, this approach can lead to numerical instability and ill-conditioned design matrices. In contrast, LeverageSHAP ([Musco & Witter, 2025](#)), PolySHAP ([Fumagalli et al., 2026](#)), and our proposed OddSHAP solve the regression subject to exact constraints.

We can neatly derive these constraints for the Fourier basis. Recall that Fourier basis functions are defined as $\chi_T(S) = (-1)^{|S \cap T|}$.

The Empty Set Constraint: For $S = \emptyset$, the intersection $|S \cap T| = 0$ for all T . Thus, $\chi_T(\emptyset) = 1$ for all basis functions. The constraint $\hat{f}(\emptyset) = f(\emptyset)$ implies:

$$\sum_{T \in \mathcal{T}} \beta_T \chi_T(\emptyset) = \sum_{T \in \mathcal{T}: |T| \text{ even}} \beta_T + \sum_{T \in \mathcal{T}: |T| \text{ odd}} \beta_T = f(\emptyset). \quad (27)$$

The Full Set Constraint: For $S = [d]$, the intersection is simply T . Thus, $\chi_T([d]) = (-1)^{|T|}$. The basis function evaluates to 1 if $|T|$ is even and -1 if $|T|$ is odd. The constraint $\hat{f}([d]) = f([d])$ implies:

$$\sum_{T \in \mathcal{T}} \beta_T \chi_T([d]) = \sum_{T \in \mathcal{T}: |T| \text{ even}} \beta_T - \sum_{T \in \mathcal{T}: |T| \text{ odd}} \beta_T = f([d]). \quad (28)$$

In our restricted regression setting (OddSHAP), we seek to minimize the use of even-order terms. We satisfy the necessary degrees of freedom by including exactly one even coalition in our support: the empty set $T = \emptyset$. Under this construction, $\sum_{|T| \text{ even}} \beta_T$ simplifies to just β_\emptyset .

Adding Equation (27) and Equation (28) yields the solution for the intercept:

$$2\beta_\emptyset = f([d]) + f(\emptyset) \implies \beta_\emptyset = \frac{f([d]) + f(\emptyset)}{2}. \quad (29)$$

Subtracting Equation (28) from Equation (27) yields the constraint on the odd coefficients:

$$2 \sum_{T \in \mathcal{T}: |T| \text{ odd}} \beta_T = f(\emptyset) - f([d]) \implies \sum_{T \in \mathcal{T}: |T| \text{ odd}} \beta_T = -\frac{f([d]) - f(\emptyset)}{2}. \quad (30)$$

C.3. Constrained Optimization via Projection

By explicitly fixing β_\emptyset and deriving the sum constraint on the odd coefficients (Equation (30)), we transform the original problem into a constrained least squares problem on the odd terms only:

$$\hat{f} = \underset{\beta \in \mathbb{R}^{|\mathcal{T}|-1}: \langle \beta, \mathbf{1} \rangle = -\frac{f([d]) - f(\emptyset)}{2}}{\operatorname{argmin}} \sum_{S: \emptyset \subset S \subset [d]} w_{|S|} \left(f(S) - \frac{f([d]) + f(\emptyset)}{2} - \sum_{T \in \mathcal{T}} \chi_T(S) \beta_T \right)^2. \quad (31)$$

We solve this efficiently by projecting the problem. Geometrically, Equation (30) restricts the solution to a hyperplane defined by the normal vector $\mathbf{1}$ (the all-ones vector). We project the regression target and design matrix onto the subspace orthogonal to $\mathbf{1}$, solve the unconstrained regression in this projected space, and then map the solution back to satisfy the sum constraint.

This approach guarantees that the efficiency property holds exactly, regardless of the sampling budget m . Even when $m \ll 2^d$, our estimator prioritizes the exact evaluation of $f(\emptyset)$ and $f([d])$, ensuring the resulting Shapley values sum to the correct total payoff.

D. Further Experimental Results

In this section, we provide further experimental details and results. All experiments were conducted on a consumer-grade laptop with an 11th Gen Intel Core i7-11850H CPU and 30GB of RAM.

D.1. Total Runtime of Approximation Algorithms

Figure 5 reports the total runtime (median with IQR) for all approximators across different budgets (m). We observe that the runtime of OddSHAP is similar to RegressionMSR, whereas MSR, LeverageSHAP and Permutation Sampling are generally faster. Moreover, the runtime of OddSHAP and LeverageSHAP substantially increases for larger budgets.

Figure 6 reports the runtime in seconds for different components (sampling, proxy fit, extraction, regression) of OddSHAP across different budgets (m).

Sampling The *sampling* is based on the `CoalitionSampler` implemented in the `shapiq` library, and uses rejection sampling. [Witter et al. \(2025b\)](#) have proposed a more efficient method, which could optimize runtime in future implementations.

Proxy Fitting the *proxy* yields a moderate increase in the runtime of OddSHAP. The LightGBM ([Ke et al., 2017](#)) proxy scales well to both, higher number of samples and higher number of features.

Extraction In cases where $m < d \cdot \eta$, OddSHAP directly extract the Shapley values from the GBT, which is the main driver of computational costs. After m passes this threshold, we observe that ProxySPEX efficiently extract the most influential Fourier interactions, which results in a drop in runtime of *extraction*. This component then stabilizes over time.

Regression The *regression* component of OddSHAP is used when $m \geq d \cdot \eta$, and remains small when the number of samples is small. However, with larger budgets, the regression component becomes a substantial driver in the runtime of OddSHAP, confirming our theoretical observations. With budgets over 10,000 samples, the total runtime and regression runtime are almost identical on the log scale.

D.2. Runtime Analysis in Simulated Settings

Figures 7 to 10 report the runtime using a simulated setting, where the cost of evaluating a single subset in f was set to $T_1 \in \{0.001, 0.01, 0.1, 1\}$. Naturally, we observe that the differences in observed in raw runtime from Figure 5 have stronger impact when T_1 is small. However, even in the lowest cost setting with $T_1 = 0.001$ we do not observe changes in the state-of-the-art performance of OddSHAP. For $T_1 = 1$, we observe curves, which are almost identical to Figure 2 with transformed x-axis.

D.3. Ablation Study on Number of Interactions

In Figure 11, we report the ablation on varying budget $m \in \{5000, 10000, 20000\}$ samples. In all cases, particularly for the Estate value function, adding interaction terms yields performance increases compared with LeverageSHAP (OddSHAP without interactions). If η is too small ($\eta = 2$), we observe a pattern similar to overfitting, which decreases the performance, since there is not enough budget to accurately fit each interaction term. Lastly, for larger budgets, we observe stronger performance gains using interactions in OddSHAP.

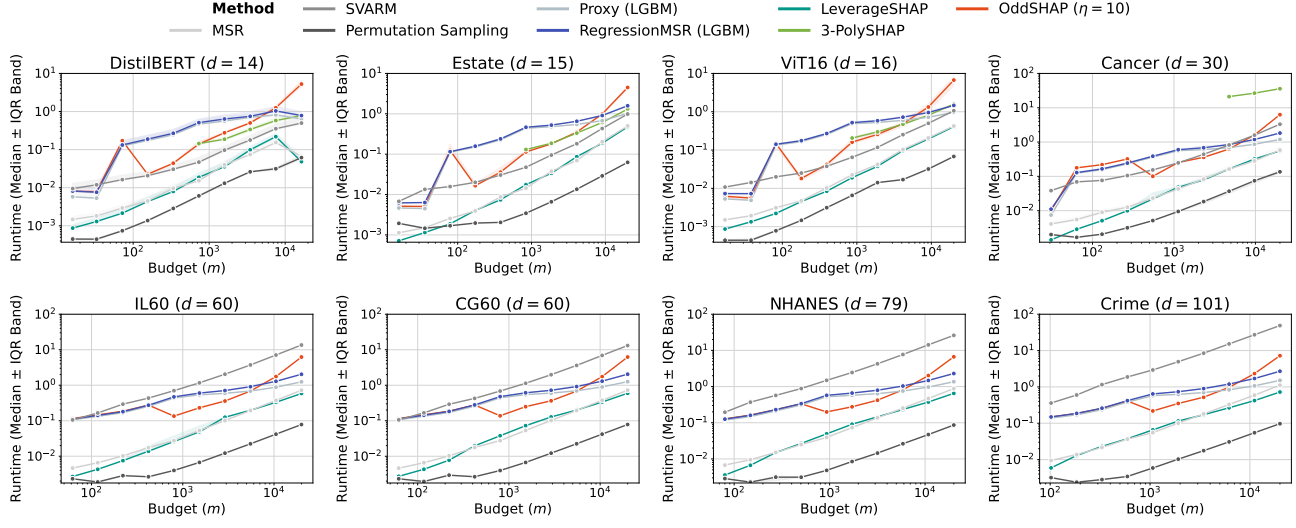


Figure 5. Runtime measured in seconds (median and IQR band) for varying budgets (m). OddSHAP has similar runtime compared with RegressionMSR, but higher runtime than LeverageSHAP.

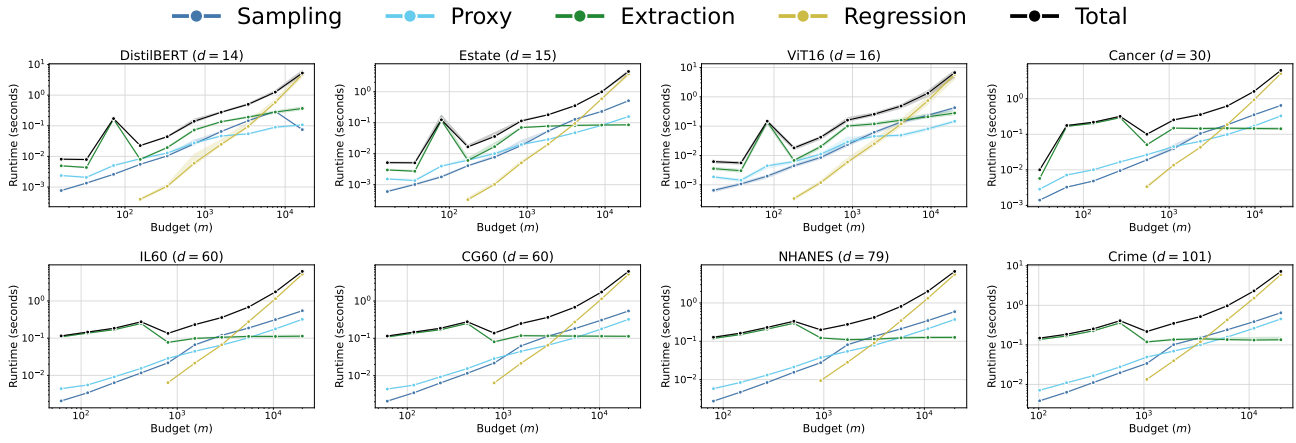


Figure 6. Median runtime with interquartile range (IQR) band for components of OddSHAP. All computations have a fairly small impact on runtime, where the polynomial regression is the leading factor for larger budgets

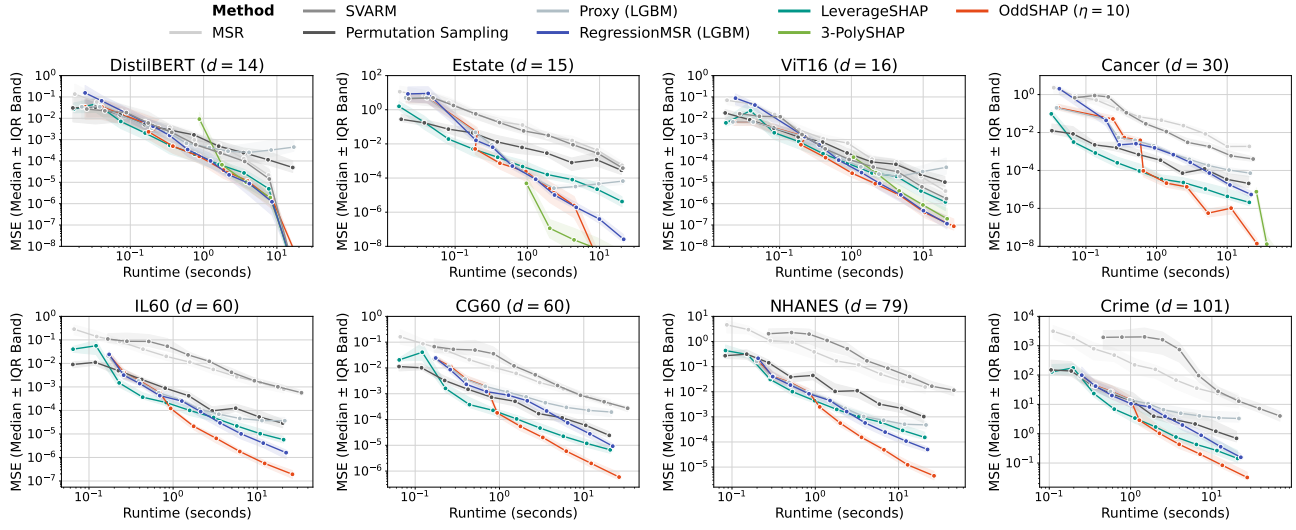


Figure 7. Approximation quality measured by MSE (median and interquartile range (IQR) band) for different runtimes with evaluation cost of 0.001 seconds.

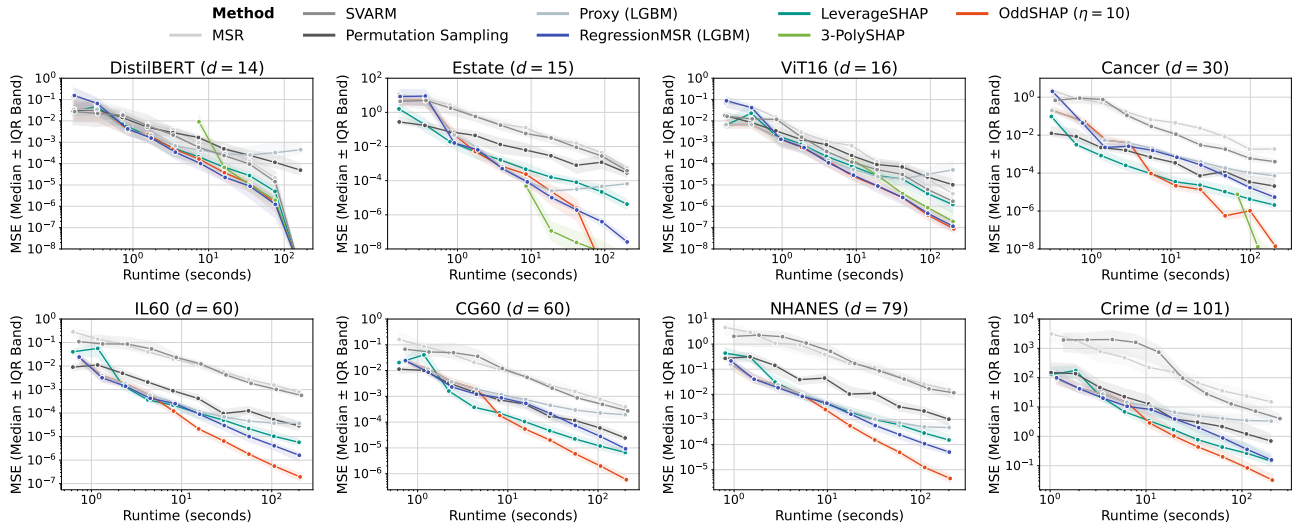


Figure 8. Approximation quality measured by MSE (median and interquartile range (IQR) band) for different runtimes with evaluation cost of 0.01 seconds.

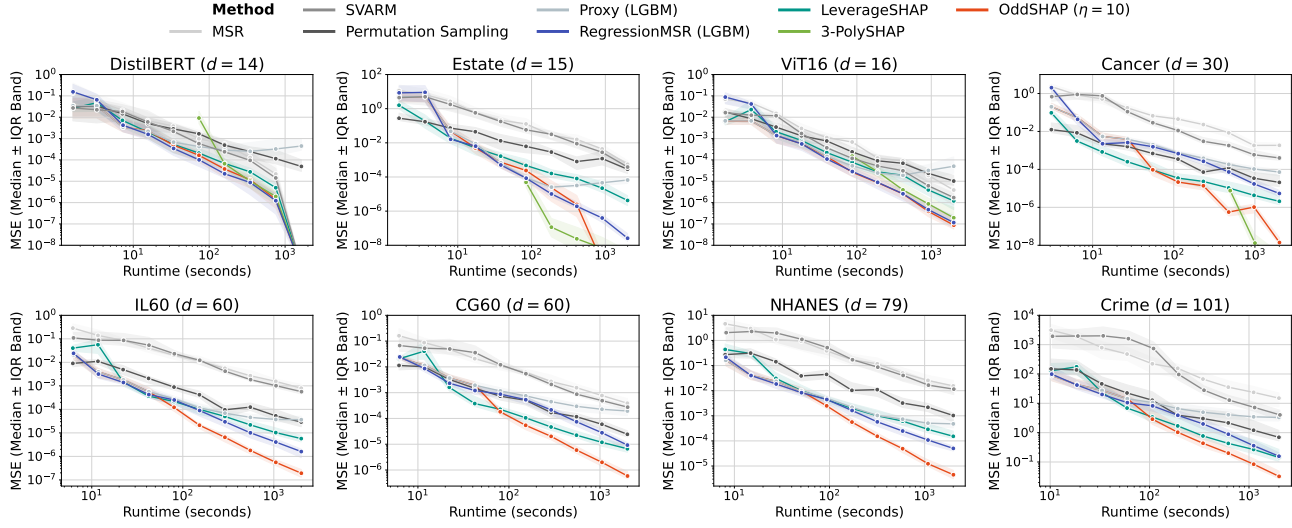


Figure 9. Approximation quality measured by MSE (median and interquartile range (IQR) band) for different runtimes with evaluation cost of 0.1 seconds.

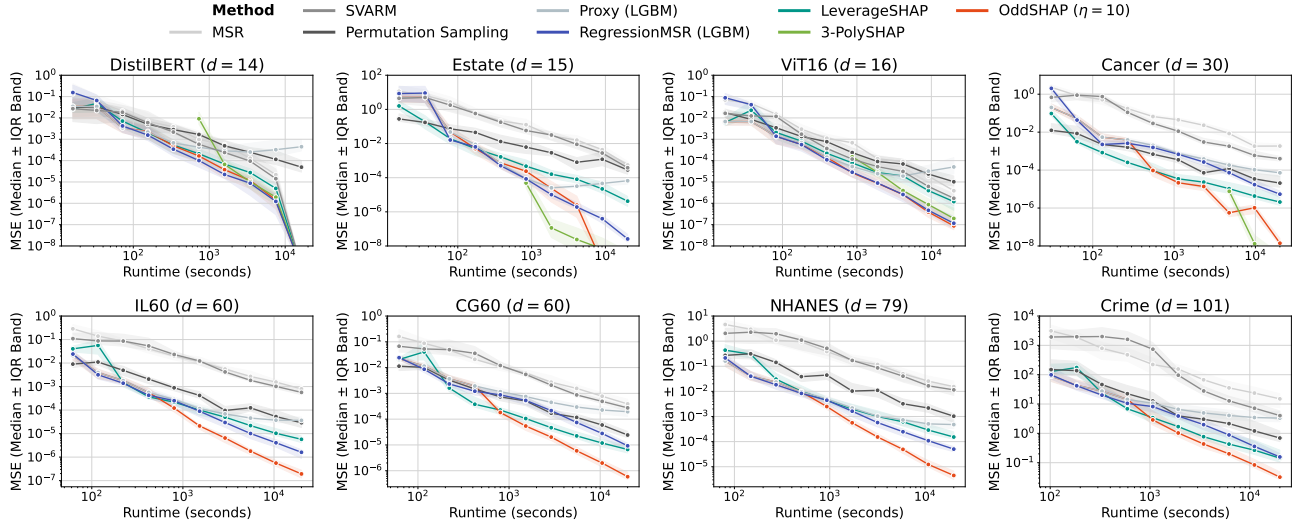


Figure 10. Approximation quality measured by MSE (median and interquartile range (IQR) band) for different runtimes with evaluation cost of 1 seconds

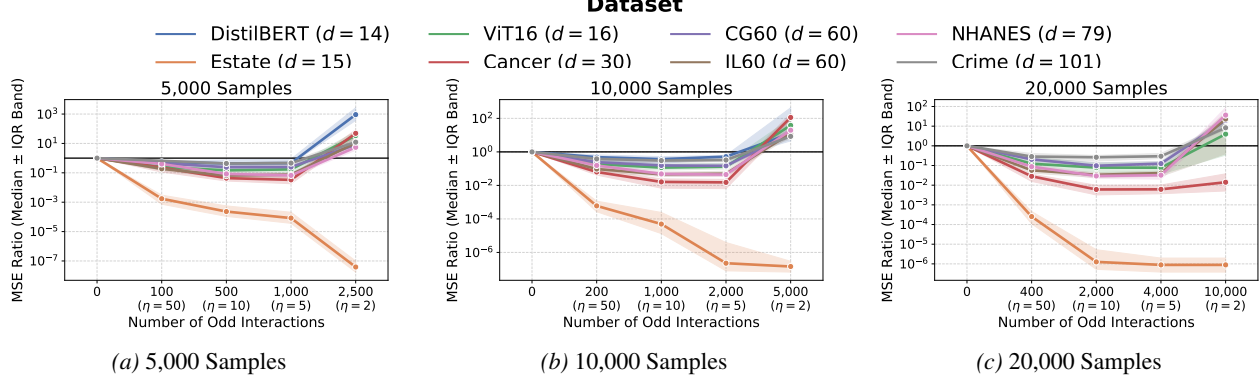


Figure 11. MSE Ratio (Median ± IQR Band) comparing Shapley MSE to base regression (no interactions) for different choices of k interactions under (left) 5,000 samples, (center) 10,000 samples, and (right) 20,000 samples.